Magnetotelluric three-dimensional forward modeling by meshfree point interpolation method

LI Jun-jie, Zhang hong-gang, Zhu Hong-lei

(Zhejiang Design Institute of Water Conservancy and Hydroelectric Power, Hangzhou Zhejiang 310002, China)

Email：lijunjiecsu@163.com.

Abstract. As an important supplement and development of mesh method numerical calculation, meshfree method is a kind of new numerical algorithm in last decade. Point interpolation method(PIM), as a simple and efficient meshfree method, avoids the mesh generation and has obtained many good results in the field of computational mechanics. This paper devotes PIM to magnetotelluric three-dimensional forward modeling, introduces the approximate principle of PIM in detail, and deduces the discrete system matrix expression which corresponding to the magnetotelluric three-dimensional variational problem by combining the Galerkin method and the gauss integral formula, then the boundary conditions of loading technique is briefly introduced. The effectiveness of three-dimensional PIM is verified by the numerical calculation of several models.

1. Introduction

Mesh method such as integral equation method(IEM)[1-2], finite difference method(FDM)[3-4] and finite element method(FEM)[5-8] are usually used for magnetotelluric three-dimensional forward. They have their own advantages and disadvantages respectively: Calculation process of FDM seem directly, but it can not handle complex geophysical models; the split and quadrature process of IEM only in abnormal body domain, hence IEM does not involve complex issues of absorbing boundary like differential method, has the features of efficiency and convenience in three-dimensional electromagnetic numerical simulation, however the same as FDM, it can not cope with calculation of complex subsurface physical properties and boundaries models. FEM is suitable for the calculation of complex distribution of physical properties and boundary shapes, its biggest flaw is that when solving complex models mesh generation appears difficulty. Meshfree method[9] as a complement and development for FEM which emerged in the field of computational mechanics in last decade is a new class of numerical algorithms, its physical properties is loaded on the gauss points which only related with coordinate location, so it can adapt the calculation of complex model under the rules of distribution node. Element-free Galerkin method(EFGM)and point interpolation method(PIM) as two kinds of mature global weak-form meshfree method have been successfully applied to two-dimensional forward modelling of seismic wave field[10], radar electromagnetic field[11] and MT field[12-14]. The results showed global weak-form meshfree method have the advantages of high precision and convenient model loading. However, PIM applied to magnetotelluric three-dimensional forward has not been reported.

This paper devotes PIM to MT three-dimensional forward, introduces the shape function constructing process of three-dimensional PIM, derives the overall matrix expression of PIM corresponding to MT three-dimensional variational problem, briefly describe the three-dimensional

gauss integration technology containing background grid, finally the effectiveness of PIM is verified through numerical calculation of several models.

2. MT three-dimensional variational problem

Assuming in Cartesian coordinate system, origin point locates at the surface of earth, which Z axis points down, X axis points the East and Y axis points the North. Solution domain V is a hexahedron area with ABCD and EFGH as clockwise coding in the upper surface Γ_u and lower surface Γ_d respectively. Γ_e is the boundary of surface and air(Fig 1).

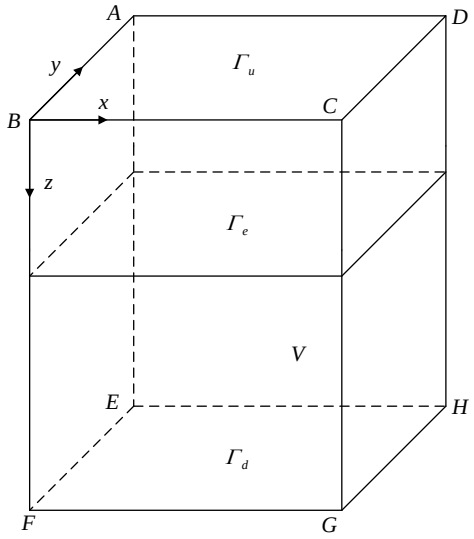

Figure 1 MT three-dimensional model

When the earth electrical structure is three-dimensional, the following variational problem is satisfied[8]

$$\begin{cases} \delta F(\boldsymbol{E}) = \int_V [\nabla \times \delta \boldsymbol{E} \cdot \nabla \times \boldsymbol{E} - k^2 \boldsymbol{E} \cdot \delta \boldsymbol{E}] \mathrm{d}V + \int_{\Gamma_d} kE_x \cdot \delta E_x \Gamma_d + \int_V \nabla \cdot \boldsymbol{E} \mathrm{d}V = 0 \qquad \Gamma_d \in EFGH \\ E_x = 1, E_y = 0, \ E_z = 0 \qquad\qquad \Gamma_u \in ABCD \end{cases} \tag{1}$$

Where ∇ is three-dimensional Hamiltonian operator, $\nabla = \frac{\partial}{\partial x}\boldsymbol{e}_x + \frac{\partial}{\partial y}\boldsymbol{e}_y + + \frac{\partial}{\partial z}\boldsymbol{e}_z$, $k = \sqrt{-\mathrm{i}\omega\mu\sigma}$, ω is angular frequency, μ is permeability, ε is permittivity and σ is conductivity.

3. MT three-dimensional variational problem solved by meshfree method

3.1 support domain

Shape function of PIM is constructed by the nodes which locates in support domain. Support domain is an artificially drawn area, its concept is similar to element in FEM. Hexahedron and sphere are commonly shape of support domain. Any gauss point X_Q , its support domain size d is determined by

$$d = \alpha d_c \tag{2}$$

Where α is the support domain dimensionless size, the accuracy and efficiency of meshfree method reduces with increasing support domain dimensionless size α, the optimal α value is 1.0 to 1.2 for MT forward[12], d_c is the nodal spacing near the point $\boldsymbol{X}_Q$ which could be determined by

$$d_c = \frac{\sqrt[3]{B}}{\sqrt[3]{n}-1} \tag{3}$$

Where B is the area of the estimated support domain, n is the number of nodes covered by the domain with the dimension of B. When nodes uniformly distribute, d_c could be defined as nodal spacing. In this paper, hexahedron support domain is adopted, the support domain sizes of x direction, y direction and z direction are following

$$\begin{cases} d_x = \alpha_x d_{cx} \\ d_y = \alpha_y d_{cy} \\ d_z = \alpha_z d_{cz} \end{cases} \tag{4}$$

where d_{cx}, d_{cy} and d_{cz} are the nodal spacing of x, y and z direction respectively. α_x , α_y and α_z are the corresponding support domain dimensionless size. For convenience the paper sets $\alpha_x = \alpha_y = \alpha_z = \alpha = 1.0$, in this case , the support domain size equals the element in FEM.

3.2 Construction of shape functions in PIM

Consider a continuous function $u(\boldsymbol{X})$ defined in a domain *Ω*, which is represented by a set of field nodes. The $u(\boldsymbol{X})$ at a point of interest $\boldsymbol{X}$ is approximated in the form of

$$u^h(\boldsymbol{X}) = \sum_{j=1}^{m} p_j(\boldsymbol{X}) a_j = \boldsymbol{p}^{\mathrm{T}}(\boldsymbol{X})\boldsymbol{a} \tag{5}$$

where $\boldsymbol{p}(\boldsymbol{X})$ is three-dimensional polynomial basis function in the space coordinates $\boldsymbol{X}^{\mathrm{T}} = [x, y, z]$, $\boldsymbol{a}$ is the coefficient, and *m* is the number of monomials for $\boldsymbol{p}(\boldsymbol{X})$ which is built by Pascal's triangles, its linear basis functions is given by

$$\boldsymbol{p}^{\mathrm{T}}(\boldsymbol{X}) = \{1 \quad x \quad y \quad z \quad xy \quad xz \quad yz \quad xyz\}$$

Equation (5) can be written in the following matrix form

$$\boldsymbol{U} = \boldsymbol{P}\boldsymbol{a} \tag{6}$$

where $\boldsymbol{U} = \{u_1\ u_2\ u_3 \cdots u_n\}^{\mathrm{T}}$, $\boldsymbol{a} = \{a_1\ a_2\ a_3 \cdots a_n\}^{\mathrm{T}}$, the expansion of $\boldsymbol{P}$ is Equation (7)

$$\boldsymbol{P} = \begin{bmatrix} 1 & x_1 & y_1 & z_1 & x_1y_1 & x_1z_1 & y_1z_1 & x_1y_1z_1 \\ 1 & x_2 & y_2 & z_2 & x_2y_2 & x_2z_2 & y_2z_2 & x_2y_2z_2 \\ 1 & x_3 & y_3 & z_3 & x_3y_3 & x_3z_3 & y_3z_3 & x_3y_3z_3 \\ \vdots & \vdots & \vdots & \vdots & \vdots & \vdots & \vdots & \vdots \\ 1 & x_8 & y_8 & z_8 & x_8y_8 & x_8z_8 & y_8z_8 & x_8y_8z_8 \end{bmatrix} \tag{7}$$

Because of the number of nodes and basis functions are always equal ($m = n = 8$) in PIM, Equation (7) is hence a square matrix form, coefficient $\boldsymbol{a}$ can be obtained through matrix inverse operation

$$\boldsymbol{a} = \boldsymbol{P}^{-1}\boldsymbol{U} \tag{8}$$

Substituting Equation (8) back into Equation (5)

$$u^h(\boldsymbol{X}) = \boldsymbol{p}^{\mathrm{T}}(\boldsymbol{X})\boldsymbol{P}^{-1}\boldsymbol{U} = \sum_{i}^{n} \phi_i u_i = \boldsymbol{\Phi}^{\mathrm{T}}(\boldsymbol{X})\boldsymbol{U} \tag{9}$$

where $\boldsymbol{\Phi}^{\mathrm{T}}(\boldsymbol{X})$ is a vector of shape functions defined by PIM

$$\boldsymbol{\Phi}^{\mathrm{T}}(\boldsymbol{X})=\boldsymbol{p}^{\mathrm{T}}(\boldsymbol{X})\boldsymbol{P}^{-1}=\left\{\phi_1(\boldsymbol{X})\ \ \phi_2(\boldsymbol{X})\ \ \phi_3(\boldsymbol{X})\ \cdots\ \phi_n(\boldsymbol{X})\right\} \tag{10}$$

Because of the PIM shape function is of polynomial form, the derivatives of the shape functions can be easily obtained like Equation (11)

$$\boldsymbol{\Phi}^{(k)}(\boldsymbol{X})=\frac{\partial^k\left[\boldsymbol{p}^{\mathrm{T}}(\boldsymbol{X})\right]}{\partial x^k}\boldsymbol{P}^{-1}=\left\{\phi_1^{(k)}(\boldsymbol{X})\ \ \phi_2^{(k)}(\boldsymbol{X})\ \ \phi_3^{(k)}(\boldsymbol{X})\ \cdots\ \phi_n^{(k)}(\boldsymbol{X})\right\}^{\mathrm{T}} \tag{11}$$

3.3 Construction of discrete systems equations in meshfree method

Magnitude E_x, E_y, E_z as three components of magnitude $\boldsymbol{E}$ in the calculation point could be described with the form of shape function multiplied field value of nodes as follow

$$\begin{cases}
E_x=\left[\phi_1\ \ \phi_2\cdots\ \phi_n\right]\left[E_{x1}\ \ E_{x2}\cdots\ E_{xn}\right]^{\mathrm{T}}=\boldsymbol{\Phi}_{(1\times n)}\boldsymbol{E}_{x(n\times 1)}=\sum_I^n\phi_I E_{xI}\\
E_y=\left[\phi_1\ \ \phi_2\cdots\ \phi_n\right]\left[E_{y1}\ \ E_{y2}\cdots\ E_{yn}\right]^{\mathrm{T}}=\boldsymbol{\Phi}_{(1\times n)}\boldsymbol{E}_{y(n\times 1)}=\sum_I^n\phi_I E_{yI}\\
E_z=\left[\phi_1\ \ \phi_2\cdots\ \phi_n\right]\left[E_{z1}\ \ E_{z2}\cdots\ E_{zn}\right]^{\mathrm{T}}=\boldsymbol{\Phi}_{(1\times n)}\boldsymbol{E}_{z(n\times 1)}=\sum_I^n\phi_I E_{zI}\\
\delta E_x=\boldsymbol{\Phi}_{(1\times n)}\delta\boldsymbol{E}_{x(n\times 1)}=\sum_I^n\phi_I\delta E_{xI}\\
\delta E_y=\boldsymbol{\Phi}_{(1\times n)}\delta\boldsymbol{E}_{y(n\times 1)}=\sum_I^n\phi_I\delta E_{yI}\\
\delta E_z=\boldsymbol{\Phi}_{(1\times n)}\delta\boldsymbol{E}_{z(n\times 1)}=\sum_I^n\phi_I\delta E_{zI}
\end{cases} \tag{12}$$

Where $\boldsymbol{\Phi}$ is shape function matrix constructed by PIM, n is the number of nodes, and $\boldsymbol{E}_x, \boldsymbol{E}_y, \boldsymbol{E}_z$ are nodes vector in support domain, Equation (13) is got by substituting Equation (12) into Equation (1)

$$
\begin{cases}
\int_V [\nabla\times\delta\boldsymbol{E}\cdot\nabla\times\boldsymbol{E}-k^2\boldsymbol{E}\cdot\delta\boldsymbol{E}]\mathrm{d}V=\delta\boldsymbol{E}\boldsymbol{K}_1\boldsymbol{E} \\
\boldsymbol{K}_1=\sum_I^N\sum_J^N\sum_k^N\int_V \begin{bmatrix} \frac{\partial\phi_I}{\partial y}\frac{\partial\phi_J}{\partial y}+\frac{\partial\phi_I}{\partial z}\frac{\partial\phi_J}{\partial z}-k^2\phi_I\phi_J & -\frac{\partial\phi_I}{\partial y}\frac{\partial\phi_J}{\partial x} & -\frac{\partial\phi_I}{\partial z}\frac{\partial\phi_J}{\partial x} \\ -\frac{\partial\phi_I}{\partial x}\frac{\partial\phi_J}{\partial y} & \frac{\partial\phi_I}{\partial x}\frac{\partial\phi_J}{\partial x}+\frac{\partial\phi_I}{\partial z}\frac{\partial\phi_J}{\partial z}-k^2\phi_I\phi_J & -\frac{\partial\phi_I}{\partial z}\frac{\partial\phi_J}{\partial y} \\ -\frac{\partial\phi_I}{\partial x}\frac{\partial\phi_J}{\partial z} & -\frac{\partial\phi_I}{\partial y}\frac{\partial\phi_J}{\partial z} & \frac{\partial\phi_I}{\partial x}\frac{\partial\phi_J}{\partial x}+\frac{\partial\phi_I}{\partial y}\frac{\partial\phi_J}{\partial y}-k^2\phi_I\phi_J \end{bmatrix}\mathrm{d}V \\
\int_{\Gamma_d} kE_x\cdot\delta E_x\Gamma_d=\delta\boldsymbol{E}\boldsymbol{K}_2\boldsymbol{E} \\
\boldsymbol{K}_2=\sum_I^N\sum_J^N\sum_k^N\int_{\Gamma_d}\begin{bmatrix} k\phi_I\phi_J & 0 & 0 \\ 0 & 0 & 0 \\ 0 & 0 & 0 \end{bmatrix}\mathrm{d}\Gamma \\
\int_V \nabla\cdot\boldsymbol{E}\mathrm{d}V=\delta\boldsymbol{E}\boldsymbol{K}_3\boldsymbol{E} \\
\boldsymbol{K}_3=\sum_I^N\sum_J^N\sum_k^N\int_V\begin{bmatrix} \frac{\partial\phi_I}{\partial x}\frac{\partial\phi_J}{\partial x} & \frac{\partial\phi_I}{\partial x}\frac{\partial\phi_J}{\partial y} & \frac{\partial\phi_I}{\partial x}\frac{\partial\phi_J}{\partial z} \\ \frac{\partial\phi_I}{\partial y}\frac{\partial\phi_J}{\partial x} & \frac{\partial\phi_I}{\partial y}\frac{\partial\phi_J}{\partial y} & \frac{\partial\phi_I}{\partial y}\frac{\partial\phi_J}{\partial z} \\ \frac{\partial\phi_I}{\partial z}\frac{\partial\phi_J}{\partial x} & \frac{\partial\phi_I}{\partial z}\frac{\partial\phi_J}{\partial y} & \frac{\partial\phi_I}{\partial z}\frac{\partial\phi_J}{\partial z} \end{bmatrix}\mathrm{d}V
\end{cases}
\tag{13}
$$

Equation (1) can finally represent the form of Equation (14) through Equation (13)

$$\delta\boldsymbol{E}\boldsymbol{K}\boldsymbol{E}=\delta\boldsymbol{E}(\boldsymbol{K}_1+\boldsymbol{K}_2+\boldsymbol{K}_3)\boldsymbol{E}=0 \tag{14}$$

Equation (14) is MT three-dimensional systems equation constructed by PIM. The expression of $\boldsymbol{K}$ contain quadrature in solving domian V and its boundary Γ, it could be solved by Gauss quadrature. For example, the elements locate in the upper left corner of $\boldsymbol{K}_1$ and $\boldsymbol{K}_2$, their quadrature could be represented as the sum of unit integral as follow.

$$
\begin{cases}
K_{IJ}=\sum_k^{n_c}\sum_{i=1}^{n_g}\omega_i\left\{[\frac{\partial\phi_I}{\partial y}\frac{\partial\phi_J}{\partial y}+\frac{\partial\phi_I}{\partial z}\frac{\partial\phi_J}{\partial z}]-k^2(\boldsymbol{X}_{Qi})\phi_I\phi_J\right\}|J_{ik}^D| \\
K_{IJ}=\sum_k^{n_c}\sum_{i=1}^{n_g}\omega_i k(\boldsymbol{X}_{Qi})\phi_I\phi_J|J_{ik}^D|
\end{cases}
\tag{15}
$$

where n_c and $n_{c\Gamma}$ are, respectively, the total number of background grid and boundary grid. n_g and $n_{g\Gamma}$ are, respectively, the total number of Gauss points in the quadrature domain and the boundary of quadrature domain. J_{Qi}^D and J_{Qi}^B are the corresponding Jacobian matrices, ω_i is the Gauss weighting factor for Gauss point $\boldsymbol{X}_{Qi}$.

Boundary conditions need to be loaded before solving linear equations $\boldsymbol{K}\boldsymbol{U}=0$, although boundary conditions of PIM can be loaded directly, program design seems more troublesome, therefore, this paper uses penalty function method to load boundary conditions, diagonal elements

K_{II} in the stiffness matrix turns to αK_{II}, α is the penalty coefficient, its value can be 10^4~10^{10}, then using the $\boldsymbol{E}$ value of the boundary to replace the right side zero vector of the equation.

4. Numerical calculation

In order to verifies the effectiveness of PIM algorithm, several numerical models are calculated. Model 1 is three-layer medium model: the resistivity of first layer $\rho_1 = 500\Omega \cdot \mathrm{m}$, layer thickness is 1km. The resistivity of second layer $\rho_2 = 2000\Omega \cdot \mathrm{m}$, layer thickness is 3km. The resistivity of third layer $\rho_3 = 100\Omega \cdot \mathrm{m}$, layer thickness is 2.5km, air layer thickness is 500m. Nodes are equally spaced in solving domain, total the number of (11×11×71) nodes and (10×10×70) background grids, node spacing is $100\mathrm{m}$. Model 2 is hexahedral low resistance model, background resistivity is $1000\Omega \cdot \mathrm{m}$,abnormal body resistivity is $100\Omega \cdot \mathrm{m}$, length, width, height of abnormal body is 400m, depth of abnormal body is 600m, the center axis projection of abnormal body corresponds to the origin of solving domain，total the number of (31×31×51) nodes, node spacing is 200m, air layer thickness is 2000m.

Figure 2 are numerical results of PIM for three-layer medium model, as shown in figure 2, the calculation results of PIM are consistent with analytical solutions, the correctness of algorithm is verified. Figure 3 is the calculation results of model 2 by PIM when frequency is 10Hz, apparent resistivity profile and impedance phase profile present minimum in the central area and present maximum in both sides of the minimum(Fig 3), both of them better reflect the existence of underground abnormal body, the effectiveness of PIM for MT three-dimensional forward is further highlighted.

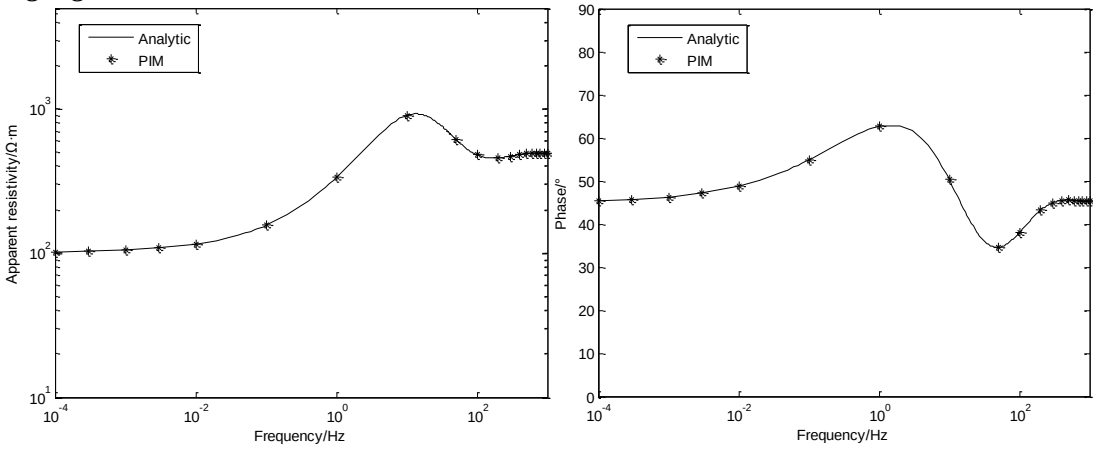

Figure 2 Calculation results of PIM for three-layer medium model

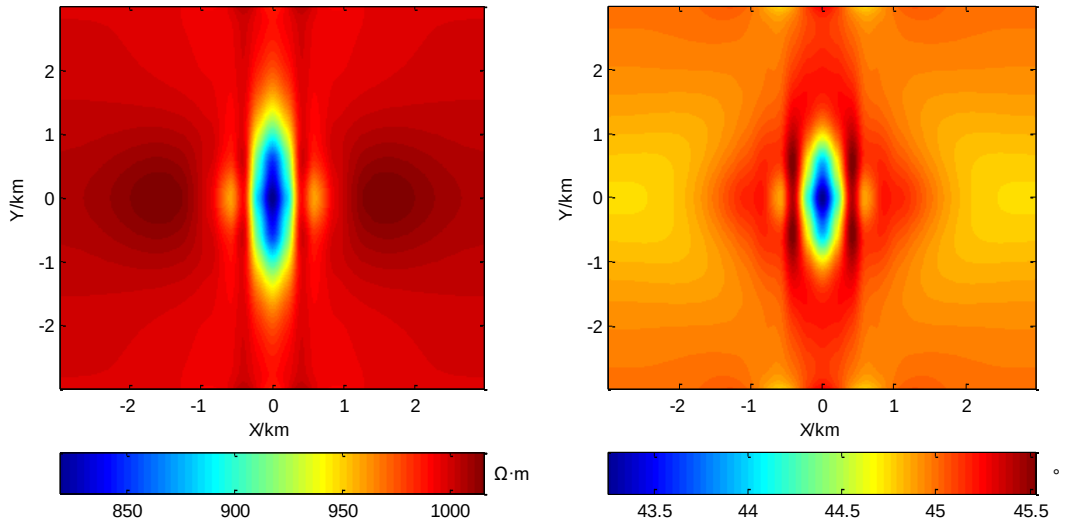

Figure 3 Calculation results of model 2 by PIM for when frequency is 10Hz

5. Conclusion

PIM is successfully applied to magnetotelluric three-dimensional forward, the construction process of three-dimensional shape functions of PIM is introduced in detail, and the discrete system matrix expression which corresponding to the magnetotelluric three-dimensional variational problem is deduced, then three-dimensional gauss integration technology containing background grid and the boundary conditions of loading technique are briefly described.

The calculation results of apparent resistivity and impedance phase for three-layered medium model are all consistent with analytical solutions, the response characteristics of surface electromagnetic in 10Hz frequency also better reflect the existence of three-dimensional abnormal body, the effectiveness of algorithm is verified.

Acknowledgments

This work was supported by the National Natural Science Foundation of China (40874055) and the Natural Science Foundation of Hunan Province (14JJ2012)

References

[1] Garbon H, Zhdanov M S 2002 Comtraction intergral equation method in three-dimensional electromagnetic modeling[J]. *Radio Science,* **37**(6): 1089-1101.
[2] XU Kai-jun, LI Tong-lin 2006 Three-dimensional magnetotelluric forward modeling using integral equation[J]. *Northwestern Seismological Journal,* **28**(2): 104-107.
[3] SHEN Jin-song 2003 Modeling of 3D electromagnetic responses in frequency domain by using staggered grid finite difference method[J]. *Chinese Journal of Geophysics,* **46**(2): 281-288.
[4] CHEN Hui, DENG Ju-zhi, TAN Han-dong 2011 Study on divergence correction method in three-dimensional magnetotelluric modeling with staggered-grid finite difference method[J]. *Chinese Journal of Geophysics,* **54**(6): 1649-1659.
[5] HUANG Lin-ping, DAI Shi-kun 2002 Finite element calculation method of 3D electromagnetic field under complex condition[J]. *Earth Science-Journal of China University of Geosciences,* **27**(6): 775−779.
[6] Mitsuhata Y, Uchida T 2004 3D magnetotelluric modeling using the T-Omega finite-element method[J]. *Geophysics*, **69**(1): 108-119.
[7] LIU Chang-sheng, TANG Jing-tian, REN Zheng-yong, FENG De-shan 2010 Three-dimension magnetotellurics modeling by adaptive edge finite-element using unstructured meshes[J].

Journal of Central South University (Science and Technology), **41**(5): 1855-1859.
[8] TONG Xiao-zhong, LIU Jian-xin, XIE Wei, 2009 Three-dimensional forward modeling for magnetotelluric sounding by finite element method[J]. *Journal of Central South University of Technology,* **16**(1): 136−142.
[9] LI Jun-jie,YAN Jia-bin 2014 Developments of meshless method and applications in geophysics[J]. *Progress in Geophysics,* **29**(1): 452-461.
[10] JIA Xiao-feng , HU Tian-yue, WANG Run-qiu 2006 A mesh-free algorithm of seismic wave simulation in complex medium[J]. *Oil Geophysical Prospecting,* **41**(1): 43-48
[11] FENG De-shan, WANG Hong-hua, DAI Qian-wei 2013 Forward simulation of Ground Penetrating Radar based on the element-free Galerkin method[J]. *Chinese Journal of Geophysics,* **56**(1): 298-308.
[12] YAN Jia-bin, LI Jun-jie 2014 Magnetotelluric forward calculation by meshless method[J]. *Journal of Central South University (Science and Technology),* **45**(10): 3513-3520.
[13] Li Jun-jie, Yan Jia-bin 2015 Magnetotelluric two-dimensional forward by finite element-radial point interpolation method[J]. *The Chinese Journal of Nonferrous Metals,* **25**(5): 1314-1324.
[14] Li Jun-Jie, Yan Jia-Bin, Huang Xiang-yu 2015 Precision of meshfree methods and application to forward modeling of two-dimensional electromagnetic sources[J]. *Applied Geophysics,* **12**(4): 503-515.